ACS APPLIED MATERIALS & INTERFACES

Research Article

www.acsami.org

Poly(ester amide)s from Soybean Oil for Modulated Release and Bone Regeneration

Janeni Natarajan,[†] Queeny Dasgupta,[‡] Shreya N. Shetty,[§] Kishor Sarkar,[§] Giridhar Madras,[‡,§] and Kaushik Chatterjee*[,‡,∥]

[†]Centre for Nano Science and Engineering, [‡]Centre for Biosystems Science and Engineering, [§]Department of Chemical Engineering, and [∥]Department of Materials Engineering, Indian Institute of Science, Bangalore 560012, India

Supporting Information

ABSTRACT: Designing biomaterials for bone tissue regeneration that are also capable of eluting drugs is challenging. Poly(ester amide)s are known for their commendable mechanical properties, degradation, and cellular response. In this regard, development of new poly(ester amide)s becomes imperative to improve the quality of lives of people affected by bone disorders. In this framework, a family of novel soybean oil based biodegradable poly(ester amide)s was synthesized based on facile catalyst-free melt-condensation reaction. The structure of the polymers was confirmed by FTIR and ^{1}H -NMR, which indicated the formation of the ester and amide bonds along the polymer backbone. Thermal analysis revealed the amorphous nature of the polymers. Contact angle and swelling studies proved that the hydrophobic nature increased with increase in chain length of the diacids and decreased with increase in molar ratio of sebacic acid. Mechanical studies proved that Young's modulus decreased with decrease in chain lengths of the diacids and increase in molar ratio of sebacic acid. The in vitro hydrolytic degradation and dye release demonstrated that the degradation and release decreased with increase in chain lengths of the diacids and increased with increase in molar ratio of sebacic acid. The degradation followed first order kinetics and dye release followed Higuchi kinetics. In vitro cell studies showed no toxic effects of the polymers. Osteogenesis studies revealed that the polymers can be remarkably efficient because more than twice the amount of minerals were deposited on the polymer surfaces than on the tissue culture polystyrene surfaces. Thus, a family of novel poly(ester amide)s has been synthesized, characterized for controlled release and tissue engineering applications wherein the physical, degradation, and release kinetics can be tuned by varying the monomers and their molar ratios.

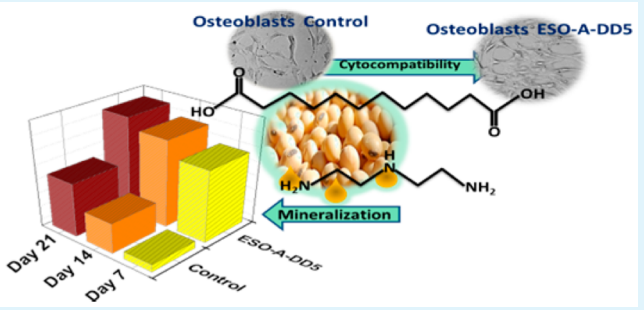

KEYWORDS: *soybean oil, biodegradable, poly(ester amide)s, drug delivery, cytocompatible, mineralization*

1. INTRODUCTION

The multidisciplinary field of bone tissue regeneration is a burgeoning alternative for autologous bone grafts that promises cure for millions of people affected by musculo-skeletal disorders worldwide. However, the translation of bone tissue regeneration practices from bench to bedside remains a formidable task.[1] The last few decades have witnessed the emergence of a palette of biomaterials as promising scaffolds that support cell growth. Synthetic biodegradable polymers have become a subject of research in the field of drug delivery and tissue engineering due to their wide range of beneficial properties including enhanced cell growth.[2,3] Developing a polymeric biomaterial encompassing properties such as biodegradability, biocompatibility, and optimal mechanical properties mimicking bone and also capable of eluting molecules that boost the overall regenerative capacity of cells[2,4] has become the prime focus to recreate a physiological native environment.

A trending family of polymers for usage in biomedical applications is the class of poly(ester amide)s (PEAs). Any polymer possessing both ester and amide linkages in its chain backbone can be considered as a poly(ester amide).[5] Therefore, PEAs present synergistic properties of degradability similar to polyesters and thermo-mechanical properties similar to polyamides.[6,7] Due to these properties, development of novel PEAs for biomedical applications becomes crucial. PEAs reported to date have been prepared by various mechanisms such as melt polycondensation,[8] solution polycondensation,[9] and interfacial polycondensation[10] but have limitations such as purification and low molecular weight.[11,12]

A multitude of factors such as low cost of monomers, ubiquitous availability, ease of synthesis, and other beneficial properties have instigated the unrestricted usage of polymers derived from fossil resources.[13] However, the ready availability, cost effectiveness, and eco-friendly features of vegetable oils make them a viable alternative renewable resource.[14,15] Besides,

Received: August 18, 2016
Accepted: September 6, 2016
Published: September 6, 2016

DOI: 10.1021/acsami.6b10382
ACS Appl. Mater. Interfaces 2016, 8, 25170−25184

Scheme 1. Reaction Scheme for the Synthesis of the ESO-A-SA

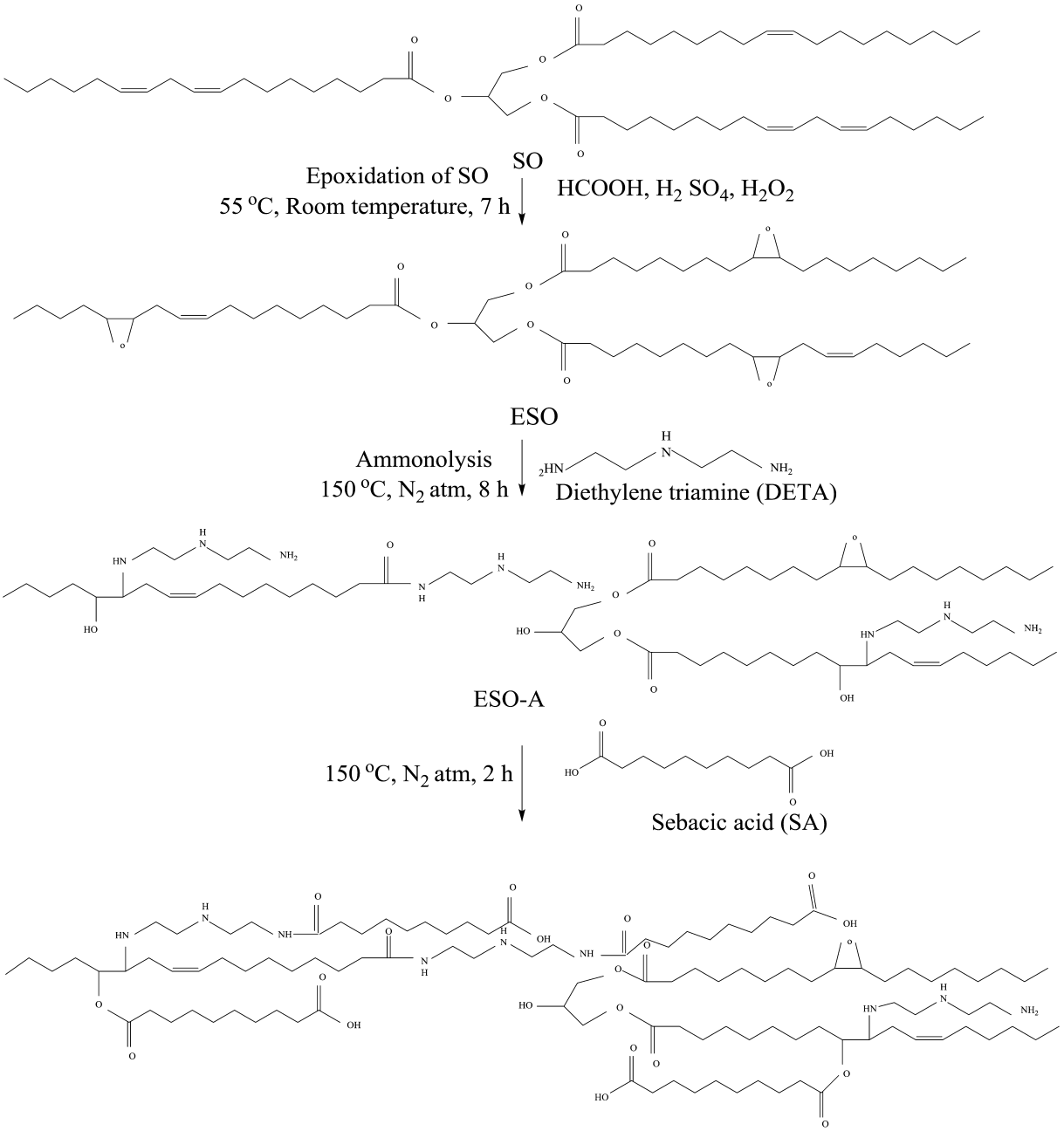

it has been elegantly demonstrated in several polymerization reactions that vegetable oils showed high reactivity as monomers.[14] The various functional groups in the oil during polymerization reactions will result in polymers of varying properties that can be used for widespread applications.[14] The sites of esters and carbon−carbon double bonds present in vegetable oils have been targeted for modification to yield a variety of monomers.[16]

Among many vegetable oils, soybean oil has received wide acceptance because of its large number of carbon−carbon double bonds thus resulting in different monomers.[17] Soybean oil offers beneficial health properties such as antiarrhythmic, anti-inflammatory, and lowering of blood pressure and cholesterol.[18] Further, the significant amount of Vitamin K present in soybean oil plays a pivotal role in bone health,[19] thus proving to be a suitable candidate for bone regeneration.

Soybean oil has been previously employed in the manufacture of lubricants, paints, soaps, bioplastics, and coatings.[20] Numerous studies of soybean oil based polyurethanes have been reported but its slow degradation rate make them unsuitable for tissue engineering scaffolds.[21] Few studies of soybean oil based polyesters have been reported for various applications.[22] The modulus and tensile strength of polyurethane elastomers depend on the ability of the hard segments to microphase-separate, which depends on the thermodynamic incompatibility between the hard and soft segments. Increasing the hydrophobicity of the soft segment generally leads to better phase separation and therefore higher modulus and

DOI: 10.1021/acsami.6b10382
ACS Appl. Mater. Interfaces 2016, 8, 25170−25184

strength.[23,24] The above factor is the prerequisite of bone tissue engineering as it has been proven that only rigid matrices stimulate cell differentiation toward osteogenic lineage.[25] Reports have evidenced that different polyurethanes possessing different properties could be obtained by tuning polyols of vegetable oil.[16,26] The easiest route to obtain polyols is the epoxidation of double bonds and subsequent reaction of the oxirane ring with polyamines, anhydrides, and polyacids to form polymers.[27−29] Wang et al. synthesized polyol-amines and cross-linked the elastomer using anhydrides for applications in rubber industries.[27] However, in this study, the polyol-amines were synthesized and further polymerized with dicarboxylic acids before thermally curing the polymer. The selection of monomers based on its non-toxicity and degradability becomes essential because biocompatibility and biodegradability are the foremost criteria of developing scaffolds. Triglycerides comprising both saturated and unsaturated fatty acids form a major portion of soybean oil.[30] Fatty acids are nearly completely eliminated from the human body by the β-oxidation pathway in the form of CO_2. The other monomers used in this study are diethylene triamine (DETA) and dicarboxylic acids (adipic, suberic, sebacic, and dodecanedioic). DETA is primarily removed via urine while dicarboxylic acids are also excreted via β-oxidation pathway.

The rationale behind this study is to exploit the beneficial traits of soybean oil and to prepare poly(ester amide)s as biodegradable polymers for tailored release. In this study, soybean oil was epoxidized and subsequently reacted with DETA to obtain polyamine-polyol and amide linkages to obtain PEA and further reacted with different dicarboxylic acids to obtain ester linkages. A series of linearly increasing chain lengths of dicarboxylic acids was selected as it was proven that diacids with different chain lengths contribute to the variation in properties of polymers.[31,32] Thermosets are preferred for their advantages such as flexibility, modulation of properties, high strength, and thermal and chemical resistances imparted due to high cross-linking density.[33] Therefore, in the final step, the polymer was cured to increase the cross-linking density to obtain thermosets. The molar stoichiometric ratios of monomers were also varied to study their effects on the properties of polymers. To the best of our knowledge, vegetable oil based poly(ester amide)s for biomedical applications have not been reported to date.

2. MATERIALS AND METHODS

2.1. Materials. Refined soybean oil (SO) was purchased from Fortune-Adani Wilmar, India. The chemicals needed to prepare epoxidized soybean oil (ESO), namely, glacial formic acid (90% pure), sulfuric acid, and hydrogen peroxide (30%) were obtained from Merck (India). DETA (Diethylene Triamine) and sebacic acid were obtained from SD. Fine Chemicals (India). Other dicarboxylic acids such as adipic acid, suberic acid, and dodecanedioic acid were procured from Sigma-Aldrich (U.S.A.). The solvent, tetrahydrofuran, was purchased from SRL Chemicals (India).

2.2. Synthesis of Epoxidized Soybean Oil (ESO). ESO was prepared based on a previous report.[34] 100 mL of SO along with 11 mL of glacial formic acid was taken in a 250 mL single neck round-bottom flask and placed in oil bath and stirred at 55 °C. To this mixture, 0.5 mL of conc. sulfuric acid was added. This was followed by the dropwise addition of 81 mL of hydrogen peroxide. The reaction was performed for 7 h. Later, the obtained product was filtered for excess water removal and subsequently washed with water to remove excess acids and neutralize the mixture. The mixture was later subjected to rotary evaporation and drying at 60 °C to obtain the final ESO (60% yield). There was a notable color change from mustard yellow to lemon yellow after epoxidation. The epoxy value of ESO was determined by the standard method of hydrochloride−acetone titration method[35] and was found out to be 6.1.

2.3. Synthesis of Poly amine−Polyol. The ring opening reaction of ESO was performed by adding DETA in a two neck 100 mL round bottomed flask at 150 °C under continuous nitrogen purging and stirring (90% yield).[27] ESO and DETA were taken in the weight ratio of 1:1 (approximately 10:1 molar ratio). The molecular weight of ESO was calculated by MALDI, as discussed later. The reaction was performed until the epoxy peak disappeared and the product started becoming jelly-like at approximately 8 h. The reaction was terminated before the product started becoming "jelly-like" and not cross-linked. This product was soluble in solvents like tetrahydrofuran. The color of the product changed to orange. The product was washed with water and dried by rota-evaporation to remove the unreacted DETA. ESO and DETA were also taken in the weight ratio of 1:0.5 to understand the effect of ester of soybean oil.

2.4. Synthesis of Poly(ester amide)s. ESO−DETA mixture of weight ratio 1:1 was further reacted with dicarboxylic acids to obtain poly(ester amides). ESO−DETA and dicarboxylic acids (adipic, suberic, sebacic, and dodecanedioic) were taken in the molar ratio of 1:5 (molecular weight of ESO−DETA calculated from MALDI). The reaction is a simple noncatalytic melt condensation reaction under nitrogen atmosphere at 150 °C for 2 h (90% yield). The final product was washed with water at a slightly higher temperature (60 °C) to remove the unreacted acids. ESO−DETA was also reacted with sebacic acid in the ratio of 1:3 and 1:7. All prepolymers (all ratios) were subjected to thermal curing at 120 °C under −700 mmHg in vacuum oven for 3 days. The reaction scheme is depicted in Scheme 1 based on a plausible structure.[37]

2.5. Nomenclature. Seven polymers were synthesized. ESO:DETA in the weight ratio of 1:0.5 will be called ESO-A0.5. ESO:DETA in the weight ratio of 1:1 is denoted as ESO-A. ESO:DETA in the weight ratio of 1:1 when further reacted with adipic (AA), suberic (SU), sebacic (SA), and dodecanedioic (DD) acids in the molar ratio of 1:5 will be hereafter referred to as ESO-A-AA5, ESO-A-SU5, ESO-A-SA5, and ESO-A-DD5, respectively. When ESO−DETA in the weight ratio of 1:1 was further reacted with sebacic acid in the molar ratio of 1:3 and 1:7 and the polymers obtained are given the nomenclature as ESO-A-SA3 and ESO-A-SA7, respectively.

2.6. Material Characterization of Polymers. NMR and MALDI characterizations were performed on the prepolymers since they require the polymers to be soluble in some solvent. The cured polymers are not soluble in any solvent. Other studies such as FTIR, DSC, contact angle, DMA, %swelling, degradation, dye release, and biological studies were performed only on the cured polymers.

2.6.1. FTIR Spectroscopy. The chemical structures of the prepolymers and cured polymers were studied using FTIR spectra. FTIR spectra were obtained by using Attenuated total reflectance (U-ATR) mode. All spectra were recorded with a signal average of 12 scans using a resolution of 4 cm^{-1} within the range of 600−4000 cm^{-1} (PerkinElmer Frontier FT−NIR/MIR spectrometer).

2.6.2. ^{1}H-NMR Spectroscopy. ^{1}H-NMR (proton-nuclear magnetic resonance) was performed for the representative compounds such as SO, ESO, ESO-A0.5, ESO-A-AA5, and ESO-A-SA5 using Bruker Avance NMR Spectrometer (400 MHz). They were dissolved in deuterated d6-DMSO (ESO-A0.5, ESO-A-AA5, and ESO-A-SA5) and $CDCl_3$ (SO and ESO) that were calibrated against internal standards. ESO-A0.5 was chosen since it was not further reacted with acids but contains ester present in the glycerol center of soybean oil. ESO-A-AA5 and ESO-A-SA5 were chosen to show the effect of different dicarboxylic acids with linearly increasing chain lengths. NMR was not performed for different molar ratios of sebacic acid such as ESO-A-SA3 and ESO-A-SA7 since there might be differences in peaks only related to methylene protons.[27] The ^{13}C NMR cross-polarization/magic angle spinning (CP/MAS) spectrum of ESO-A-SA5 was recorded on a Bruker AV-500 solid state spectrometer operating at a 125.6 MHz Larmor frequency. Glycine is used as an external standard to establish the cross-polarization Hartmann−Hahn condition. The polymer was placed in a zirconia rotor and was operated in a spinning speed of 12

DOI: 10.1021/acsami.6b10382
ACS Appl. Mater. Interfaces 2016, 8, 25170−25184

kHz. A total of 12 000 scans were obtained using the (CP/MAS) technique. The spectra were acquired with a proton $\pi/2$ pulse length of 4 μs, 5 s recycle delay time, with a 2000 μs contact time.

2.6.3. Determination of Molecular Weight. Matrix-assisted laser desorption/ionization spectroscopy (MALDI TOF MS) was performed to calculate the molecular weight of the polymers (UltrafleXtreme MALDI Bruker Daltonics). *N*,*N*-Dimethylformamide (DMF)/acetonitrile mixture was used to dissolve the samples. MALDI TOF MS was performed on ESO to calculate the molecular weight of ESO and approximately the number of double bonds that have been epoxidized. ESO-Amine in the weight ratio of 1:1 was chosen for analysis to calculate the molecular weight and to proceed for the further steps. MALDI TOF MS was also performed on the ESO-A reacted with the dicarboxylic acids.

2.6.4. Differential Scanning Calorimetry. Differential scanning calorimetry (DSC) was performed to study the thermal characteristics of the polymers (TA Instruments Q 2000). Samples of 3 to 5 mg were loaded onto the aluminum pans. Later, heating and cooling cycles from −50 to 200 °C under nitrogen flow of 50 mL/min at the rate of 10 °C min^{-1} were performed. Second heating cycles were considered for analysis in all cases.

2.6.5. Dynamic Mechanical Analysis. Dynamic mechanical analysis (DMA) was used to analyze the mechanical properties of the cured polymers (TA Instruments, Q 800). Films of dimensions (30 × 5 × 1 mm^3) were used for the studies. A uniform thermal frequency sweep of 1 to 10 Hz at 37 °C was employed. Additional operational conditions used were 15 μm amplitude, 0.01 N preload and film/fiber tension clamps.

2.6.6. Surface Water Wettability. Contact angle goniometry (Data Physics) was employed to characterize the surface water wettability. One μL ultrapure water droplet was placed on the flat surface of the polymer for the readings after the droplet attained stability. Mean ± standard deviation of three independent readings were calculated, and the final data are presented.

2.6.7. %Swelling Measurement. Swelling−deswelling characteristics of the polymers were exploited to measure the %swelling of the polymers. The circular polymer samples (4.5 × 1 mm^2) (W_1) were immersed in 100 mL volume of non- solvent (acetone) at 37 °C for 12 h. Later, the samples were removed after swelling and weighed without drying (W_2). This was followed by drying in hot air oven for 12 h at 60 °C. These weights of deswelled polymers were noted as W_3 which will be equivalent to W_1. The formula for measuring %swelling can be written as follows:

$$\%\text{swelling} = (W_2 - W_3)/W_3 \times 100 \quad (1)$$

2.6.8. In Vitro Hydrolytic Polymer Degradation. Circular samples punched of dimensions (4.5 × 1 mm^2) similar to swelling studies were inserted inside the nylon meshes and later placed in 20 mL phosphate buffer saline (PBS) (pH = 7.4). They were further transferred to an incubator shaker that maintains 37 °C and shakes at 100 rpm. The samples were removed, rinsed with water, and dried in hot air oven for 12 h. The weight losses of samples were noted at predetermined time points. PBS replenishment was provided every 24 h to avoid the changes occurring due to pH.

The percentage weight loss of the samples was determined based on the differences between the initial weight and the dry weight of the samples after immersing in PBS. The formula can be written as follows:

$$\%\text{mass loss} = (M_o - M_t)/M_o \times 100 \quad (2)$$

In eq 2, M_o is the dry mass of the polymer disc before degradation, and M_t is the dry mass after immersing in PBS at fixed time points. The weight loss was also monitored at different pH conditions of 3.4 and 10.4.

2.6.9. Dye Release. Two dyes, namely, hydrophilic dye (Rhodamine B, RB) and a hydrophobic dye (Rhodamine B base, RBB) (see Supporting Information, SI, Scheme S1) were loaded to the polymers to simulate drug release. The initial concentration of the dyes loaded inside the polymers was 5%. The prepolymers were dissolved in *N*,*N*-dimethylformamide (DMF) followed by addition of 5 wt % dyes to the mixture. The mixtures were made to undergo solvent evaporation and curing, similar to that carried out for degradation. Later, the discs of dimensions similar to degradation studies were punched.

The punched samples were submerged in 20 mL PBS (pH 7.4) and placed in incubator shaker maintaining 37 °C and 100 rpm similar to degradation studies. PBS was replaced every 24 h. 100 μL PBS containing dye was aliquoted from each sample at predetermined times for 1 week. Later, the absorbance values of dyes were obtained via well plate reader at the wavelength of 553 nm. The release of dyes was monitored for 1 week. Subsequently, the samples were immersed in NaOH solution to completely extract the dye entrapped inside the polymer after 1 week of release. The fractional release was then calculated from the total amount of dye. The concentration of the dyes released was calculated from the earlier obtained calibration curves. The cumulative dye release profiles were finally obtained in the case of both the dyes.

2.6.10. Cytocompatibility of the Polymer. To assess the potential use of these polymers for bone tissue regeneration, MC3T3-E1 subclone 4 mouse preosteoblast cell line (ATCC, U.S.A.) was used to evaluate their cytocompatibility.[36] The cells (twentieth passage) were expanded in T-75 flasks with alpha-minimum essential medium (α-MEM, Sigma, U.S.A.) encompassing fetal bovine serum (10% v/v, Gibco, Life Technologies) and 1% antibiotics (Sigma) were harvested using 0.25% trypsin with EDTA for this study. Cells were maintained at 37 °C in a 5% CO_2 incubator.

2000 cells suspended in 200 μL medium were seeded onto each well of 96 well plate. The cells were left undisturbed for 12 h for attachment. Concurrently, circular samples (UV sterilized for 1 h) were immersed in 5 mL culture medium and allowed to degrade to collect conditioned medium. The discs in quadruplicate of each polymer type were submerged individually in centrifuge tubes and they were moved to CO_2 incubator (37 °C) for 24 h similar to degradation and release experiments described above. After 24 h, the culture medium was replaced with conditioned medium. The discs were placed individually in each centrifuge tubes, and they were maintained in a CO_2 incubator and 37 °C for 24 h similar to in vitro degradation and release experiments. Cytocompatibility was assessed following the exposure of the cells to conditioned medium for 24 and 72 h. Cells treated with fresh culture medium in lieu of the conditioned medium were used as the control for these experiments. The morphology and viability of the cells were also studied following the exposure of the cells to conditioned medium for 1 day and 3 days.

The cell viability was assessed by WST-1 assay. ESO-A-AA5, ESO-A-SU5, ESO-A-SA5, and ESO-A-DD5 were tested. Each well corresponded to each polymer disc (n = 4 polymer type × 4 replicates = 16 + 4 wells for control = 20 × 2 time points = 40 wells in total). WST reagent with the concentration for each well of 10 μL/100 μL medium was added to all wells. The well plate was incubated for 1 h until the color of the medium changed to yellow followed by reading the absorbance values at the wavelength of 440 nm.

The cell viability was also confirmed by the LIVE/DEAD Viability/Cytotoxicity Assay Kit (Molecular Probes, Invitrogen). Cells were stained with the concentration of 2 mM Calcein to stain live cells and 4 mM ethidium homodimer to stain dead cells at 37 °C for 15 min in CO_2 incubator and imaged using fluorescence microscope (Olympus).

Cell morphology was studied by fixing the cells using 3.7% formaldehyde (Merck) for 15 min. The fixed cells were washed using PBS and imaged microscopically in bright field (Olympus).

2.6.11. Mineralization Studies Using Alizarin Red Staining. The ability of the polymers to support osteogenic differentiation of these polymers was evaluated by studying the mineralization deposits. MC3T3-E1 cells were grown on ESO-A-DD5 circular discs in a 48-well plate, as this polymer showed slower degradation and possessed higher modulus among the other polymers of this study. Cell culture was carried out in complete culture media, as described above, along with additional supplements that are known to induce osteogenic differentiation, namely, β glycerol phosphate (10 mM) and ascorbic acid (25 μM) (Sigma).[37] Mineral deposits of calcium and phosphate were studied on day 7, day 14, and day 21. The cells were initially fixed

DOI: 10.1021/acsami.6b10382
ACS Appl. Mater. Interfaces 2016, 8, 25170−25184

at these aforementioned time intervals for 20 min at 37 °C using 3.7% formaldehyde. Filtered alizarin red dyes (200 μL) (ARS, Sigma) were added to each well later to quantify calcium deposits. The samples were incubated with the dye for 25 min in room temperature. This was followed by numerous water washes until the water became clear to remove the unbound dye. Subsequently, 0.2 mL 5% SDS in 0.5 HCl was added to each well for dissolving the AR dye for another 25 min. The optical density values were obtained by reading at 405 nm. EDX (Energy dispersive X-ray) with SEM further confirmed the presence of calcium deposition.

2.6.11.1. Statistical Analysis. One way ANOVA coupled with Tukey's test was performed to examine the differences across various polymers and control. $p < 0.05$ were considered for significant differences.

3. RESULTS AND DISCUSSION

3.1. Synthesis of Polymers. The formation of thermoset elastomers via cross-linking is preferred as mentioned above. Attacking the glycerol center of soybean oil will result in the introduction of other functional groups that would increase cross-linking of the polymers.[27] As a result, higher molecular weight can be achieved by increased cross-linking. Ammonolysis without catalyst was performed using DETA. It was hypothesized that the reactivity of triamine is high, and it can break the glycerol center as well as react with epoxy ring. When ESO:DETA was reacted in the weight ratio of 1:0.5, the ester of soybean oil did not react completely (FTIR not shown). Breaking the glycerol center and subsequently reacting with acid enables tailoring of the properties of polymers. Complete reaction of ester occurred only in the ratio of 1:1. Therefore, the weight ratio of ESO:DETA was maintained as 1:1 ratio. This product was reacted with acids in 1:3, 1:5, and 1:7 molar ratios in case of SA and 1:5 ratio for the other acids. The amount of ester was very less in 1:3 ratio (as evident from FTIR), whereas ESO-A-SA7 showed faster degradation. Therefore, a 1:5 ratio was maintained for all polymers. The reactions were performed at 150 °C as ammonolysis increases with increase in temperature.[27] Esterification reactions were performed at 150 °C, and no significant changes were observed in the final product even when the reactions were performed at 180 °C. The synthesized prepolymers were soluble in tetrahydrofuran.

3.2. Polymer Characterization. *3.2.1. FTIR Spectroscopy.* In the FTIR spectra of SO, trans =C—H stretch peak was observed at 3008 cm^{-1}. Other peaks such as asymmetric and symmetric stretching of —CH_2 at 2922 and 2857 cm^{-1}, C=O stretching ester peak from the glycerol center at 1745 cm^{-1}, and a C—C stretching peak at 1157 cm^{-1} can also be observed. After epoxidation of SO, the =C—H stretch peak completely disappeared. A new peak at 830 cm^{-1} appeared in ESO spectra which corresponds to —C—O epoxy stretch. This indicates that double bonds had been converted to oxirane rings and epoxidation reaction had taken place.[34] Other peaks mentioned in the case of SO remained the same (Figure 1a).

ESO was reacted with amine in a weight ratio of 1:0.5. The epoxy peak at 830 cm^{-1} almost disappeared. The higher reactivity of epoxy did not allow the formation of esters in the final step if reacted with epoxy group still present in the compound. A broad O—H and N—H stretching peak can be observed at 3290 cm^{-1} indicating that ammonolysis had taken place.[27] The ester peak at 1745 cm^{-1} decreased to a greater extent explaining that glycerol center had been attacked. New peaks such as —C=O stretching of amide and —N—H bending were observed at 1647 and 1553 cm^{-1} respectively.

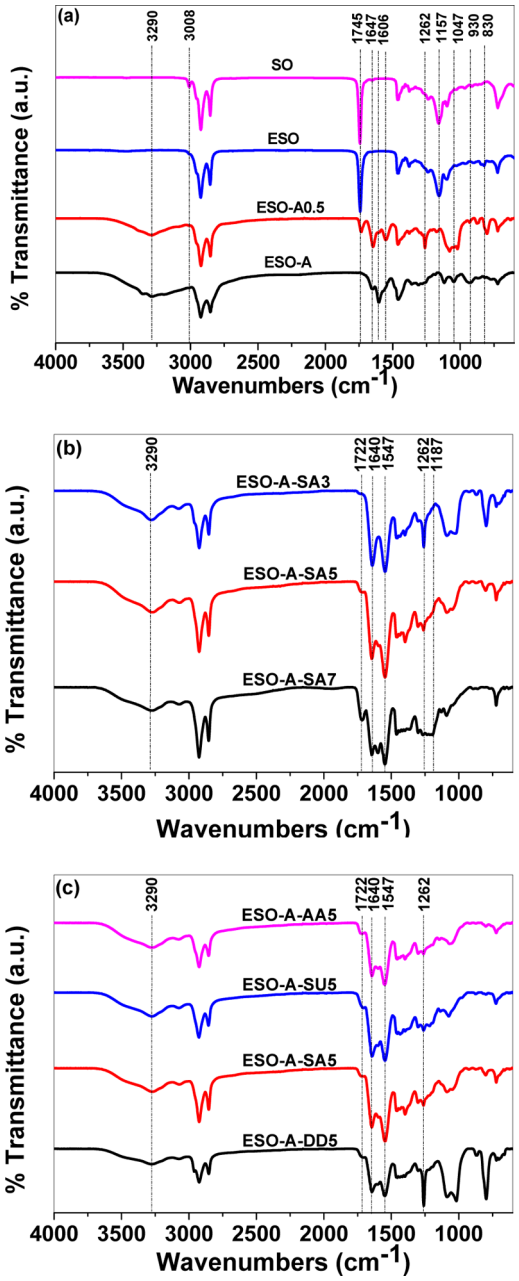

Figure 1. FTIR spectra of (a) SO, ESO, ESO-A0.5, and ESO-A; (b) ESO-A-SA3, ESO-A-SA5, and ESO-A-SA7; and (c) ESO-A-AA5, ESO-A-SU5, ESO-A-SA5, and ESO-A-DD5.

C—N amide stretching peak can be observed at 1262 cm^{-1}. A reduction in the intensity of C—O stretching at 1157 cm^{-1} can be observed due to the decrease in ester content. With increase in ratio of ESO:Amine to 1:1, the ester peak at 1745 cm^{-1} completely disappeared. C—O stretching at 1157 cm^{-1} also showed a decrease in intensity. There was an increase in the intensity of 3290 cm^{-1} peak indicating that more ammonolysis had taken place. No change was observed in the peak position of 1647 and 1547 cm^{-1}. 1606 cm^{-1} peak corresponding to —N—H bending present in DETA is more intense in ESO-A. This could be due to the presence of unreacted amines. No positional change was observed in the case of 1262 and 1157 cm^{-1} peaks (Figure 1a). This indicated that both the —OH group and —NH groups are present in the product that can be

DOI: 10.1021/acsami.6b10382
ACS Appl. Mater. Interfaces 2016, 8, 25170−25184

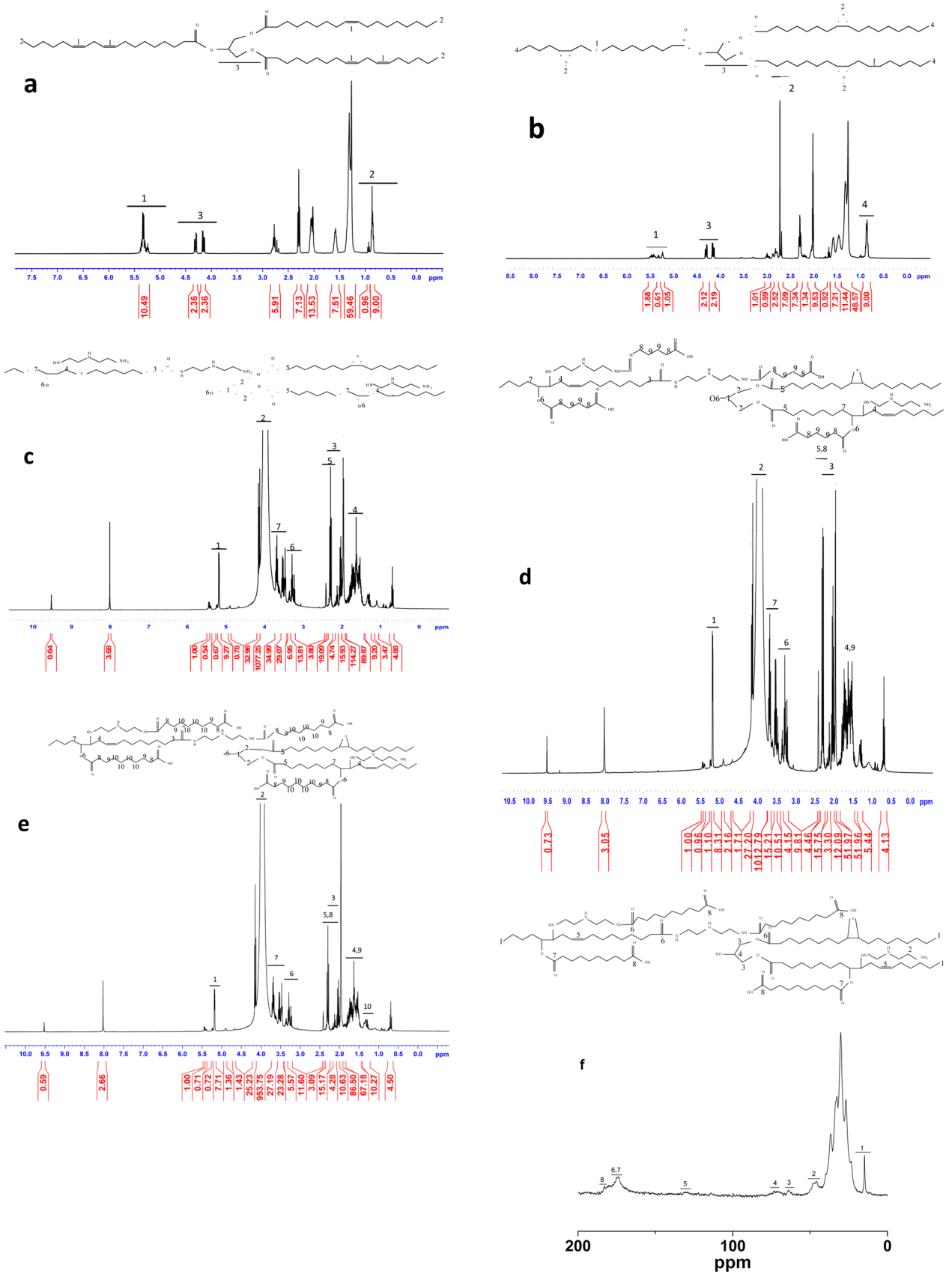

Figure 2. ^{1}H-NMR spectra of (a) SO, (b) ESO, (c) ESO-A0.5, (d) ESO-A-AA5, (e) ESO-A-SA5, and (f) 13 C spectra of ESO-A-SA5.

subsequently reacted with carboxylic acids to obtain ester amides.

When ESO:DETA in the weight ratio of 1:1 was further reacted with sebacic acid in different molar ratios of 1:3, 1:5,

DOI: 10.1021/acsami.6b10382
ACS Appl. Mater. Interfaces 2016, 8, 25170−25184

and 1:7, ester carbonyl stretch peak (—C═O) was observed at 1722 cm^{-1}.[38] With an increase in ratio of sebacic acid, the intensity of the ester peak also increased. This revealed the increase in the ester formation with an increase in molar ratio of dicarboxylic acid. Further, a decrease in intensity of the 3290 cm^{-1} peak was observed with an increase in the molar ratios of sebacic acid. This is because more N—H and O—H groups could have reacted with an increase in the molar ratio of dicarboxylic acid. The peaks related to amide at 1647, 1553, and 1262 cm^{-1} can be observed in all spectra. Additionally, a peak at 1187 cm^{-1} which is related to —C—O stretching of esters with alcohols can be observed in all spectra.[39] The intensity of this peak increased with an increase in molar ratio of dicarboxylic acid. Methylene peaks at around 2922 and 2857 cm^{-1} were also observed (Figure 1b). An additional peak around 1600 cm^{-1} in ESO-A-SA7 could be due to the presence of unreacted amines present in DETA. This confirmed the formation of both ester and amide groups in the compound.

When ESO:DETA in the weight ratio of 1:1 was further reacted with different dicarboxylic acids in the molar ratio of 1:5, all peaks mentioned earlier such as peaks at 3290, 2922, 2857, 1722, 1647, 1553, and 1262 cm^{-1} were observed in the spectra of all acids namely adipic, suberic, and dodecanedioic acids (Figure 1c).

3.2.2. ^{1}H-NMR Spectroscopy. In ^{1}H NMR spectra of SO (Figure 2a),[40] peaks around 5.4 ppm correspond to protons of double bonds. Since the integral exhibits the value of 10, it may be concluded that the number of double bonds present in soybean oil was 5. The peaks at 4.2 and 4.4 ppm could be attributed to the protons of the glycerol center. The peaks at 0.8 ppm could be ascribed to the methylene protons in the end of the molecule.

After epoxidation of soybean oil (Figure 2b),[41] the integral of the peaks around 5.4 ppm decreased from 10 to 4. This indicated that three double bonds out of five had been epoxidized. The other double bonds may not have reacted due to steric hindrance. Further, two new singlet peaks whose integrals were around 6 appeared at 2.7 ppm corresponding to epoxy protons. This corroborated the fact that three double bonds had been converted to epoxy groups. No changes in the integrals were observed for the protons attributed to the glycerol center and the methylene protons present in the end.

When ESO was further reacted with amine in the ratio of 1:0.5 (ESO-A0.5) (Figure 2c), no peaks were observed around 2.7 ppm revealing that all epoxy groups might have reacted.[27] The peaks around 5.2 ppm correspond to methine protons of glycerol center (—CH_2—C**H**—CH_2). The peaks around 4.2 ppm could be attributed toward the methylene protons of the glycerol center (—C**H$_2$**—CH—C**H$_2$**). The peaks around 2.16 ppm could be ascribed to the protons present next to the amide bond (C**H$_2$**—CO—NH). The peaks around 1.73 ppm could be correlated with the protons present between the adjacent epoxy groups. The peaks around 2.36 ppm could be corresponding to the protons adjacent to the ester groups of the glycerol center (—C**H$_2$**—COO—). The peaks around 3.23 ppm could be due to the protons of the —OH formed. Finally, the peaks between 3.5 and 3.8 ppm could be due to the protons present adjacent to the —OH groups. Thus, the formation of —OH groups and —NH groups was verified using ^{1}H-NMR which was further reacted with dicarboxylic acids to obtain esters and more amides.

When ESO:DETA in the ratio of 1:1 was reacted with dicarboxylic acid such as adipic acid (Figure 2d,e), the peaks mentioned earlier for ESO-A remained in the same position. In addition to these peaks, the peaks at 1.5 and 2.1 ppm could be ascribed to the methylene protons of adipic acid which are (COOH—CH_2—C**H$_2$**) and (COOH—C**H$_2$**—CH_2), respectively. Similar spectra were obtained when ESO-A was reacted with other dicarboxylic acids such as suberic, sebacic, and dodecanedioic acids.

As discussed earlier, while the prepolymers are soluble, the cured polymers are insoluble in solvents. In order to obtain deeper insight into the final product, solid state NMR was conducted. Figure 2f shows the solid state NMR spectra of ESO-A-SA5. The structure of ESO-A-SA5 was further confirmed using solid state ^{13}C NMR spectra.[34,42] The peak present at 14 ppm corresponds to the carbon of terminal methyl groups (—CH_3). The peaks present between 27 and 36 ppm could be correlated to all the carbons of methylene groups (—CH_2) present in the polymer. The peak at 45 ppm corresponded to carbon of methylene groups (—CH_2) adjacent to —NH_2 groups. The peak at 64 ppm could be ascribed to carbon of C—O bond adjacent to ester groups of glycerol center. The carbon of methylene groups (—CH_2) adjacent to unreacted —OH groups may be correlated to a small peak at 72 ppm. A small peak at 130 ppm could be assigned to unreacted C═C groups after epoxidation. The peaks at 173 and 174 ppm could be attributed to the carbon of C═O group of amide and ester, respectively. The peak at 182 ppm could be ascribed to the unreacted acid (C═O) present.

3.2.3. Matrix Associated Laser Desorption/Ionization (MALDI TOF MS). The average molecular weight of soybean oil is approximately 920 g/mol. The molecular weight of ESO calculated by MALDI TOF MS was 965 (see Figure S1). From the above data, it can be concluded that approximately three double bonds have been converted to epoxy groups i.e., (920 + (16 × 3) = 968). Further, the molecular weight of ESO-A was 1100. The molecular weight of the prepolymers of ESO-A-AA5 and ESO-A-SA5 were almost similar to a slight increase for polymer based on sebacic acid (1160 for ESO-A-AA5 and 1200 for ESO-A-SA5). Generally, molecular weight increases with an increase in chain length of the monomers.

3.2.4. Differential Scanning Calorimetry (DSC). Thermal characterization of polymers by DSC revealed that the synthesized polymers were completely amorphous exhibiting only glass transition temperatures (T_g) (see Figure 3, Table 1). T_g decreased consistently with an increase in molar ratio of sebacic acid and higher formation of esters. The aliphatic content also increases with esters that would increase the amorphous nature and free volume between the chains. This

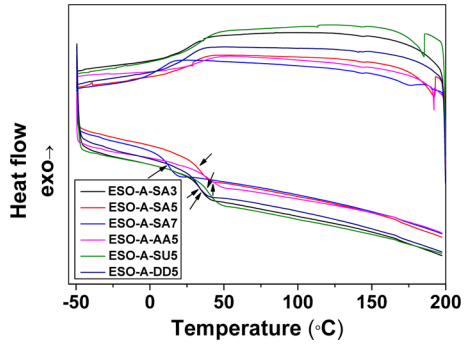

Figure 3. DSC profiles of various PEAs (both heating and cooling curves from −50 to 200 °C are shown).

DOI: 10.1021/acsami.6b10382
ACS Appl. Mater. Interfaces 2016, 8, 25170−25184

Table 1. Physical Properties, Degradation, and Dye Release Rate Coefficients, k_d and k

polymers	T_g (°C)	Young's modulus (MPa) at 10 Hz	cross-link density (n) mol/m^3	contact angle (deg)	%swelling	degradation, rate coefficient (h^{-1}) (k_d) (× 10^{-3})	RB release, k_{RB}, h^{-n} (× 10^{-3})	RBB release, k_{RBB}, h^{-n} (× 10^{-3})	k_d/k_{RB} ratio
ESO-A-SA3	35.5	60.7	0.0079	106 ± 2	2.7	13.6	25.8	25.1	0.53
ESO-A-SA5	33.4	43.9	0.0057	89 ± 1	5.8	19.3	39.5	34.8	0.49
ESO-A-SA7	12.9	35	0.0045	68 ± 2	7.8	27.5	52.9	51.7	0.52
ESO-A-AA5	42.2	15	0.0019	81 ± 1	23.2	338.4	296.5	220.1	1.14
ESO-A-SU5	38	18	0.0023	83 ± 2	18.4	160.1	159.8	139.1	1.00
ESO-A-DD5	33	121	0.0156	91 ± 2	0.5	2.8	21.2	15.5	0.13

increase in free volume reduces T_g.[43] Similar decrease in T_g was observed when sebacic acid was reacted with xylitol instead of glycerol with the same molar ratio of diamine.[44] A decrease in T_g was also observed with increase in the chain lengths of dicarboxylic acids. This is because of the formation of rigid networks when the chain length is shorter. Networks will be present far apart when the chain length of the diacids are higher and hence contributing to the increased chain mobility. This will lower T_g. Similar decrease in T_g was observed in the formation of esters based on 1,4 butane diol, succinic, and adipic acid. The ester based on adipic acid had a lower T_g when compared to succinic acid.[45] In another case of PEAs, a similar decrease in T_g was observed when sebacic acid and glycerol were reacted with a series of increasing chain lengths of diamine.[44]

3.2.5. Dynamic Mechanical Analysis (DMA). The Young's modulus was calculated from the formula which is as follows:

$$E^* = \sqrt{E'^2 + E''^2} \tag{3}$$

where E^*, E'^2, E''^2 represent the complex modulus, storage modulus and loss modulus, respectively. The complex modulus can be approximately considered as Young's modulus.[46] Mechanical properties by DMA (Table 1) exhibited that Young's modulus decreased with an increase in molar ratio of sebacic acid. The modulus value of ESO-A-SA3 is 60.7 MPa, and it decreased approximately 1.4 times to 43.9 MPa for ESO-A-SA5 and 2 times to 30 MPa in the case of ESO-A-SA7. As discussed in the previous section, since the polymers became increasingly amorphous in nature, the modulus values decreased.[47] Similar results were obtained for a PEA when 1,3-diamino-2-hydroxy propane was reacted with glycerol and sebacic acid to form PEA. The modulus values decreased from 1.5 to 1.1 MPa when the molar ratio was doubled for glycerol.[48] When the reaction was performed with different dicarboxylic acids with increasing chain lengths maintaining the same ratio, the Young's modulus values increased from 15 to 121 MPa. The modulus values were 15, 18, 43.9, and 121 MPa for ESO-A-AA5, ESO-A-SU5, ESO-A-SA5, and ESO-A-DD5, respectively. The modulus values of ESO-A-SU5 were approximately 2.5 times lesser than ESO-A-SA5. Similarly, the modulus values of ESO-A-SA5 were approximately 2.7 times lesser than ESO-A-DD5. A similar increase in trend was observed when glycerol and sebacic acid were reacted with different amines with the different chain lengths. The modulus values increased from 3 to 11.5 MPa with increase in methylene groups of the diamines.[44]

Different polymers displayed different modulus values. These modulus values fit the modulus values of both soft tissues and hard tissues. For example, the modulus value of elastin is 1.1 MPa and it is 11.8 MPa for knee cartilage.[49] ESO-AA5 and ESO-A-SU5 can be applicable for the above tissue regeneration applications. The modulus value of cancellous bone ranges from 50 to 100 MPa,[50] suggesting that ESO-A-SA5, ESO-A-SA3, and ESO-A-DD5 could be useful for bone regeneration applications.

Using the values of the calculated complex modulus, the cross-linking densities for the polymers were calculated using the following formula:[51]

$$n = \frac{E^*}{3RT} \tag{4}$$

where n is the cross-linking density, E^* represents the Young's modulus, R represents the gas constant, and T represents temperature. The temperature was kept constant (37 °C = 310 K) for all polymers. The cross-linking values increased with an increase in modulus values (Table 1). With a higher degree of cross-linking, the modulus values increase. This has been previously reported when comparison was made between poly(sorbitol-citrate-sebacate) polymers and poly(sorbitol-tartarate-sebacate) polymers.[52] For example, the cross-linking density of ESO-A-SA3 was 0.0079 mol/m^3, and it decreased to 0.0045 mol/m^3 with a decrease in modulus in the case of ESO-A-SA7. The cross-linking density value of ESO-A-SA3 was approximately 1.8 times and 1.4 times higher than that of ESO-A-SA7 and ESO-A-SA5, respectively. Similarly, with varying diacids, the cross-linking density increased with increase in chain length ranging from 0.0019 mol/m^3 to 0.0156 mol/m^3 with concomitant increase in modulus values of these polymers. The cross-linking density of ESO-A-DD5 was approximately eight times, seven times and three times higher than that of ESO-A-AA5, ESO-A-SU5 and ESO-A-SA5, respectively. The cross-linking density also plays a critical role in determining the hydrophobicity and swelling of the polymers which are discussed in the following sections.

3.2.6. Contact Angle Measurements. Contact angle measurements proved that these polymers were hydrophobic (Table 1). When comparing the data against various ratios of sebacic acid, the contact angle decreased from 106° to 68°. The hydrophobicity increased by 1.3 times from ESO-A-SA7 to ESO-A-SA5. Similarly, it increased by 1.2 times from ESO-A-SA5 to ESO-A-SA3. Similar contact angles were observed with increase in amide/ester ratio, where the contact angle decreased from 106° to 77° when dimethyl adipate and 1,4-butane diol were reacted with various ratios of amine.[53] Contact angles increase with an increase in cross-linking resulting in reduced fluid uptake.[52] This was also substantiated by cross-linking density values as discussed earlier and %swelling studies which will be discussed later. In the context of different dicarboxylic acids with increasing chain lengths, the contact angle increased with increasing chain lengths. The contact angles ranged from 81° to 91° when ESO-A was reacted with adipic acid and dodecanedioic acid. A similar increase was observed when erythritol reacted with sebacic acid and dodecanedioic acid,[54] wherein the contact angle increased from 58° to 80°. The

DOI: 10.1021/acsami.6b10382
ACS Appl. Mater. Interfaces 2016, 8, 25170−25184

reason for hydrophobicity could be attributed to the increase in methylene groups.

3.2.7. %Swelling Measurements. Swelling experiments are performed in acetone (hydrophilic nonsolvent) since the polymers will undergo hydrolytic degradation if they are exposed to water. The %swelling is dictated by the hydrophobicity and cross-linking density of the polymers. %Swelling will be higher if the polymer is hydrophilic since it allows more fluid influx.[55] In addition, the polymers will swell less if they are highly cross-linked.[56] As discussed in the previous section, the hydrophobicity increases with cross-linking density. Hence an increase in %swelling (Table 1) was found with the increase in molar ratio of sebacic acid. ESO-A-SA3 showed a %swelling of 2.7 while ESO-A-SA5 and ESO-A-SA7 showed %swelling of 5.8 and 7.8. With increase in chain lengths of diacids, the %swelling decreased. The %swelling was 23.2, 18.4, 5.8, and 0.5 for ESO-A-AA5, ESO-A-SU5, ESO-A-SA5, and ESO-A-DD5, respectively. ESO-A-DD5 had the lowest %swelling of 0.3. Similar decrease from 6.2 to 4.5 in %swelling ratio was observed when glycerol and sebacic acid were reacted with hexamethylene diamine and later with 1,12 diamino dodecane.[44] In the same family of PEA, a similar decrease was observed with increases in ratios of monomer. When glycerol and sebacic acid were reacted with 10% and 30% 1.5 diamino 2-methyl pentane, the %swelling was 7.8 and 3.6, respectively.[44].

3.3. Hydrolytic Polymer Degradation in Vitro. Hydrolytic polymer degradation was performed to test the potential for their applications in the field of drug delivery and bone tissue engineering. The degradation of the polymers should be proportionate to the time taken for the regeneration of bone. For the different molar ratios of sebacic acid (Figure 4a), the degradation of the polymers increased with increase in molar ratio of sebacic acid. In 24 h, 51%, 43% and 30% weight losses were observed in the case of ESO-A-SA7, ESO-A-SA5 and ESO-A-SA3, respectively. In 1 week, ESO-A-SA7 degraded completely, while only 95% and 89% degradation was observed in the cases of ESO-A-SA5 and ESO-A-SA3, respectively. With respect to increasing chain lengths of dicarboxylic acid, both ESO-A-AA5 and ESO-A-SU5 degraded completely within 24 h. However, only 43% and 7% degradation was observed for ESO-A-SA5 and ESO-A-DD5, respectively. The trend of different molar ratios of sebacic acid polymers can be written as follows:

ESO-A-SA7 > ESO-A-SA5 > ESO-A-SA3

The trend of different chain lengths of dicarboxylic acid polymers can be presented as follows:

ESO-A-AA5 > ESO-A-SU5 > ESO-A-SA5 > ESO-A-DD5

The above trend could be attributed toward a combination of factors such as the hydrophobicity of the polymers, %swelling, modulus values, and cross-linking densities. With an increase in the cross-linking density, the modulus and the hydrophobicity increase, whereas the %swelling decreases. The degradation of the polymer decreases with an increase in hydrophobicity since the polymer suppresses the entry of water. Both contact angle and %swelling demonstrated that the hydrophilicity increased with increase in ratio of sebacic acid and decreased with increase in chain lengths. The modulus values and cross-linking densities also decreased with an increase in the ratio of sebacic acid and increased with increase in chain lengths of diacids. Therefore, the degradation of the polymers decreased with decrease in modulus, cross-linking density, and contact angle, whereas the degradation increased with increase in %swelling. Similar decrease in degradation with increase in chain length was observed when poly(1,3-diamino-2-hydroxy propane) was reacted with glycerol and threitol, these polymers exhibited 97% and 70% weight losses in a week.[38] Similarly, when biasmide diol and 1,4-butane diol were reacted with ethane diol and butane diol, the weight losses were around 5.7% and 3.6% in 5 days, respectively.[53]

The degradation rates were modeled and calculated by applying power law kinetics,

$$-\frac{dM}{dt} = k_d M^n \tag{5}$$

In the eq 5, M stands for mass, t represents time, k_d signifies the rate coefficient corresponding to degradation, and n denotes the degradation order. The degradation data fitted first order kinetics. This signifies that the rate of the degradation is controlled by the concentration of ester bonds and is not affected by the amount of water. A plot of $-\ln (M_t/M_0)$ versus time was linear (insets of Figure 4a). k_d values based on the initial slopes with intercept being zero for all the polymers are tabulated in Table 1.

On the basis of k_d values, in the aspect of different chain lengths of diacids, it is evident that ESO-A-AA5 was the fastest degrading polymer among all polymers with rates approximately greater than two times that of ESO-A-SU5, 17 times that of ESO-A-SA5, and 120 times that of ESO-A-DD5. In the context of different molar ratios of sebacic acid, the rates of ESO-A-SA3 were approximately two times and 1.5 times lower than that of ESO-A-SA5 and ESO-A-SA7, respectively. The rate constant values of degradation followed a trend similar to that of degradation influenced by hydrophobicity. Given that a wide range of degradation rate constant values were obtained, it can

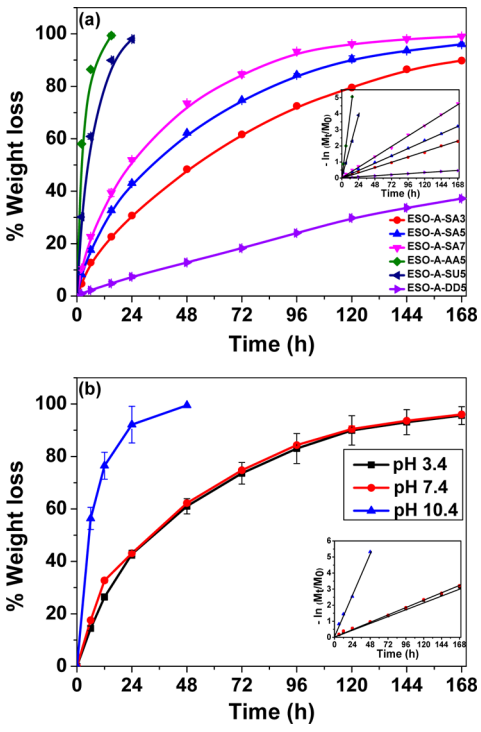

Figure 4. In vitro hydrolytic degradation profiles of (a) different PEAs in 20 mL PBS solution (pH = 7.4) (b) ESO-A-SA5 in 20 mL PBS solution in different pH (pH = 3.4, 9.4). The inset shows the variation of $-\ln (M_t/M_0)$ with time. Data points represent mean ± SD (n = 3).

DOI: 10.1021/acsami.6b10382
ACS Appl. Mater. Interfaces 2016, 8, 25170−25184

be concluded that changing the chain lengths, and the molar ratios of monomers can result in versatile polymers suitable for a multitude of biomedical applications.

3.3.1. In Vitro Hydrolytic Degradation of Polymers in Different pH. Different pH values are found in different organ systems of human body. Digestive system maintains acidic pH,[57] while basic pH is found in some chronic inflammation sites.[58] It is important to study the degradation of these polymers in different mileu since these polymers are intended to be implanted inside the body for different biomedical applications. It has also been proven that amides are not cleaved while only esters contribute for hydrolytic degradation of PEAs.[59] Esters are cleaved at a higher rate in basic pH.[60] ESO-A-SA5 was opted for this study based on the optimal degradation of this polymer. The degradation was studied in acidic pH (3.4) and basic pH (9.4) (Figure 4b). The degradation was almost similar in both acidic and neutral pH. However, the degradation was faster in basic pH. The polymer degraded completely within 48 h in basic pH while only 62% and 60% weight losses were observed in neutral and acidic pH, respectively.

Degradation in different pH data also fitted first order kinetics (inset of Figure 4b) with the k_d values being 110.7 × 10^{-3} h^{-1} and 18.7 × 10^{-3} h^{-1} for basic and acidic pH, respectively. The rate of degradation in basic environment is almost 6 times faster than that in acidic and neutral environments.

3.4. In Vitro Dye Release Studies. Biomolecules are often incorporated in polymeric scaffolds to impart bioactivity through sustained release of the molecules. To characterize the release kinetics, we assessed the release of dye that is governed primarily by the degradation of the polymer. The trend of the dye release was identical to the degradation data (Figure 5). Regarding different chain lengths of dicarboxylic acids, complete release of RB was observed in the case of ESO-A-AA5 whereas, only 84%, 24%, and 14% release of RB was observed in 48 h in the case of ESO-A-SU5, ESO-A-SA5, and ESO-A-DD5, respectively. Complete release of RB was observed in 72 h for ESO-A-SU5. In 1 week, 49% and 29% RB release was observed in the case of ESO-A-SA5 and ESO-A-DD5, respectively. Similar trend was observed in the case of RBB. Complete release of RBB was observed in 48 and 72 h in the case of ESO-A-AA5 and ESO-A-SU5 respectively. 43% and 23% release of RBB was observed in a week for ESO-A-SA5and ESO-A-DD5, respectively. In comparison across different molar ratios of sebacic acid, 73% RB release was observed for ESO-A-SA7, whereas only 47% and 31% release of RB was observed for ESO-A-SA5 and ESO-A-SA3, respectively. In the case of RBB, 70%, 43%, and 27% releases were obtained from ESO-A-SA7, ESO-A-SA5, and ESO-A-SA3, respectively. The overall trend of both RB and RBB release in the case of different molar ratios of sebacic acid can be presented as follows:

ESO-A-SA7 > ESO-A-SA5 > ESO-A-SA3

The trend of both RB and RBB related to different chain lengths of dicarboxylic acids can be written as follows:

ESO-A-AA5 > ESO-A-SU5 > ESO-A-SA5 > ESO-A-DD5

The hydrophobicity and the degradation of the polymers are the main factors that influence the dye release.[61] High modulus, high cross-linking density, and low %swelling also contribute to the overall hydrophobicity of the polymer as discussed in the earlier sections. Hydrophobicity increased with increase in chain length of dicarboxylic acids due to increase in methylene groups. The release of the dyes will be based on the water influx into the polymer from the surrounding medium. As the degradation of the polymer occurs due to the water influx, dye gets released. In addition, the release of RBB will most likely be slower than RB since it is a hydrophobic dye. The release of a hydrophobic dye from a hydrophobic polymer will be quite slower than a hydrophilic dye when placed in a hydrophilic medium. Similar trends were observed in RB and RBB loaded ESO based polyesters.[34]

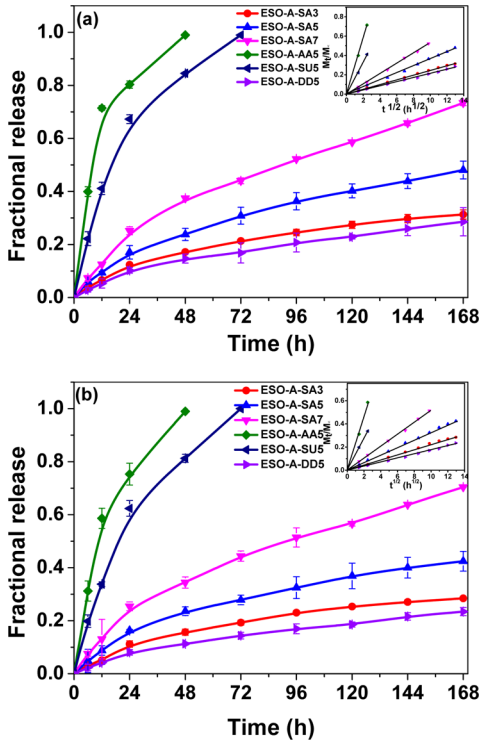

Figure 5. In vitro release of (a) hydrophilic RB dye and (b) hydrophobic RBB dye. The insets of all the plots show the variation of (M_t/M_∞) with $t^{1/2}$ $(h^{1/2})$ and the release exponent. Data points represent mean ± SD (n = 3).

The release rates were modeled using the Korsmeyer–Peppas model[62] which is as follows:

$$\frac{M_t}{M_\infty} = kt^n \tag{6}$$

In the above equation, M_t and M_∞ symbolize the concentration of the dyes released at the predetermined time period and the initial amount of dye present, while k represents the release rate coefficient, t denotes time, and n signifies the release exponent. The release rates of the dyes were fit with Higuchi kinetics. The linear plot of ln M_t/M_∞ versus ln t when n = 0.5 can be observed in the insets of Figures 5 and 6. The initial slopes of the lines were considered for k values with intercept fixed to zero in all cases (Table 1). As evident from k values, the rates of ESO-A-AA5 were 14 times higher than that of ESO-A-DD5. Similarly, the rates of ESO-A-SA7 were two times higher than that of ESO-A-SA3. This study elucidates that release rates can be tailored based on the molar ratios and chain lengths of monomers befitting a spectrum of release applications such as burst or sustained release applications. For example, treatment of wounds need an initial burst release[63] where ESO-A-AA5 or

DOI: 10.1021/acsami.6b10382
ACS Appl. Mater. Interfaces 2016, 8, 25170–25184

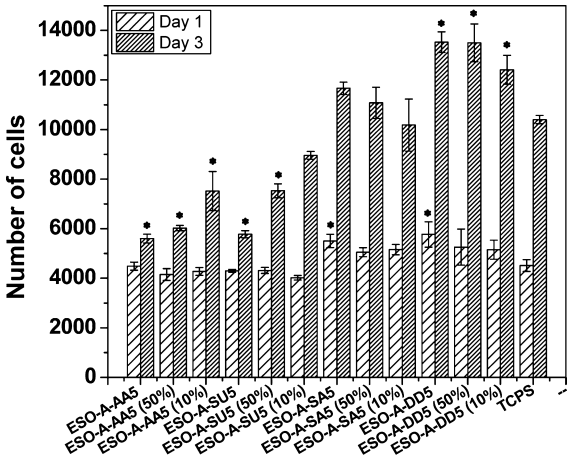

Figure 6. Cell viability of various PEAs determined by WST assay for day 1 and day 3 with various concentrations of degradation media. The * above the bars indicate that the samples are statistically significant when compared to control. Data points represent mean ± SD (n = 4).

ESO-A-SU5 can be utilized. The anti-inflammatory drugs are usually administered in a controlled manner,[64] and ESO-A-DD5 can be applicable in such sustained release applications.

The degradation profiles for the polymers (as shown in Figure 4) follow the same order as that of the release profile of the same polymers (as shown in Figure 5). However, the values are different. For example, 90% degradation of ESO-A-SA5 is observed in 1 week but only 40% release of RB is observed for the same time period. In order to investigate this further, we analyzed the FTIR spectra of the physical mixture of the dye and the polymer and compared it against that of the dye and the polymer after curing. The results indicate that —OCH_3 and —COOH groups of the dye reacts with the polymer. To quantify the interaction, the ratio of the rate constant of release of RB to the rate constant of degradation was calculated, and it was found to be 0.5 for all ESO-A-SA polymers. Further, it was 1.1 for ESO-A-AA5, 1.0 for ESO-A-SU5, and 0.1 for ESO-A-DD5. The values decreased with increase in chain lengths. The reason could be attributed to the amount of free —OH and —COOH groups present in each type of diacid varies, and hence the number of moles of dye interacting with the polymer is different with each type of polymer although the weight of the dye loaded was maintained constant.

3.5. Cytocompatibility. Testing the cytocompatibility property of the polymers that are intended for biomedical applications is of foremost importance. As the moduli of the polymers are comparable to those of the bone tissues, MC3T3-E1 mouse preosteoblasts were utilized to evaluate the ability of these polymers to support the growth of bone cells. WST assay was used to assess the cell viability in which the live cells will convert tetrazolium to water-soluble yellow formazan. Therefore, the absorbance values are directly correlated to the number of live cells based on the calibration curves. ESO-A-AA5, ESO-A-SU5, ESO-A-SA5, and ESO-A-DD5 with different diacids were chosen for the studies. The assay revealed the cytocompatible nature of the polymers (Figure 6). The cells remained attached in the presence of the conditioned media from all the polymers at day 1. ESO-A-SA5 and ESO-A-DD5 showed a number of cells higher than control (tissue culture polystyrene- TCPS). The differences were statistically significant. ESO-A-AA5 and ESO-A-SU5 showed cell numbers similar to that of control and the differences were not statistically significant from each other. The cell numbers increased on all polymers from day 1 to day 3 suggesting that these polymers were non-toxic. The number of cells doubled from approximately 5700 to 13 500 in the case of ESO-A-DD5. The cells numbers increased from 4500 to 10 400 in the case of control. The differences of ESO-A-DD5 were statistically significantly higher when compared to control. The number of cells increased from 5050 to 11 000 in the case of ESO-A-SA5. The differences were not statistically significant from control. The cell numbers also increased in the case of ESO-A-AA5 and ESO-A-SU5. The cells were lesser in number for ESO-A-AA5 and ESO-A-SU5 when compared to control and these differences were statistically significant. Although the proliferation was lesser when compared to other samples, the cell numbers increased from day 1 to day 3 indicating the non-toxicity with reduced proliferation.

The viability was also evaluated with different concentrations of the conditioned media containing degradation products by diluting them with fresh media. Thus, in addition to the above, 50% and 10% concentrations of conditioned media were investigated. On day 1, the values of the cell viability for different concentrations of conditioned media for all polymers were similar to control. The differences were not statistically significant. On day 3, the viability for both 10% and 50% of ESO-A-AA5 were statistically significantly lesser than control. However, 10% and 50% of ESO-A-DD5 showed viability higher than that of control. The effect of increased/reduced cell proliferation compared to the control by the degradation products in the conditioned media was seen to decrease with increased dilution of the conditioned medium. For all concentrations, the cell numbers increased from day 1 to day 3 indicating that the polymers were cytocompatible for all concentrations.

Cell viability was also assessed qualitatively using live/dead fluorescent images. The images substantiated the data of WST assay. The number of viable cells was higher in the case of ESO-A-DD5 and ESO-A-SA5 than on ESO-A-SU5 and ESO-A-AA5 (Figure 7). The number of viable cells was also higher for ESO-A-DD5 when compared to control. The percentage of live cells were 41%, 44%, 97%, 99.8%, and 97% in the case of ESO-A-AA5, ESO-A-SU5, ESO-A-SA5, ESO-A-DD5, and control, respectively.

Cell morphology was also evaluated since it is indicative of cell function.[65] Bright field images (Figure 8a,b) showed that the cells displayed characteristic "spindle shaped" morphology and there were no differences between all polymers and control in morphology. The cells looked healthy and well spread. Since the morphology and viability were studied after the exposure of the cells to conditioned media, it appears that the degradation products are essentially nontoxic to the cells. Therefore, these materials are suitable for further evaluation in vivo.

3.6. Osteogenic Differentiation Studies. Mineralization studies were performed to evaluate the ability of the polymers to drive the cells toward osteogenesis. The calcium deposition on the surface of the polymers was quantified using ARS (Figure 9). ARS staining showed that the calcium deposition was higher in the case of ESO-A-DD5 when compared to control. The differences were also statistically significant on days, 7, 14, and 21. In the case of ESO-A-DD5, the absorbance values increased from 0.51 to 0.69 from day 7 to day 21 whereas, in the case of control, the absorbance value was only 0.32 on day 21. This confirms that ESO-A-DD5 promotes osteogenic differentiation of the cells. SEM micrographs

DOI: 10.1021/acsami.6b10382
ACS Appl. Mater. Interfaces 2016, 8, 25170−25184

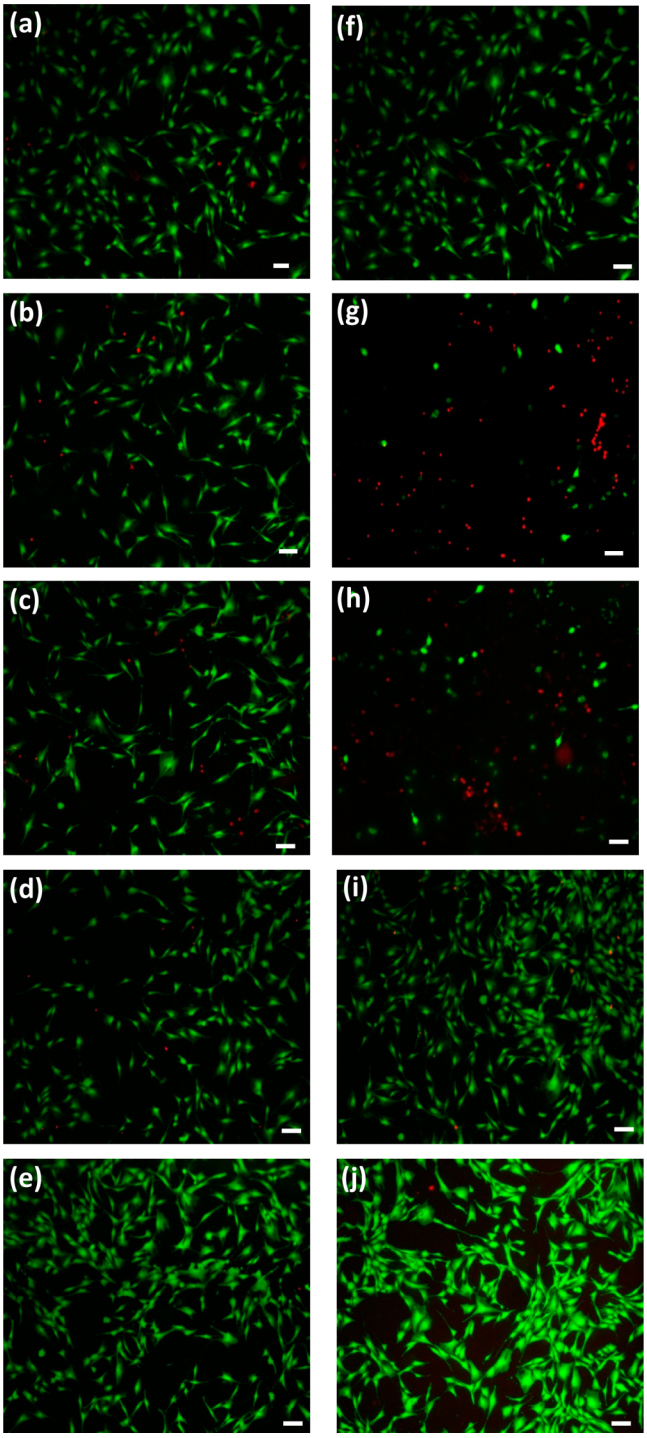

Figure 7. Fluorescent images of viability assay performed for various PEAs (a) Control day 1, (b) ESO-A-AA5 day 1, (c) ESO-A-SU5 day 1, (d) ESO-A-SA5 day 1, (e) ESO-A-DD5 day 1, (f) Control day 3, (g) ESO-A-AA5 day 3, (h) ESO-A-SU5 day 3, (i) ESO-A-SA5 day 3, and (j) ESO-A-DD5 day 3. Scale bar indicates 20 μm. All images are taken at 4x magnification. Viable cells are stained green while non-viable cells are stained red.

revealed cells exhibited the round morphology for some cells which may be attributed to the surface hydrophobicity[66] (Figure 10a). Many cells were elongated with good cell−cell communication. Calcium deposition on the surface of the polymer was also confirmed by EDX (Figure 10b). The presence of amine groups in the polymer could have promoted

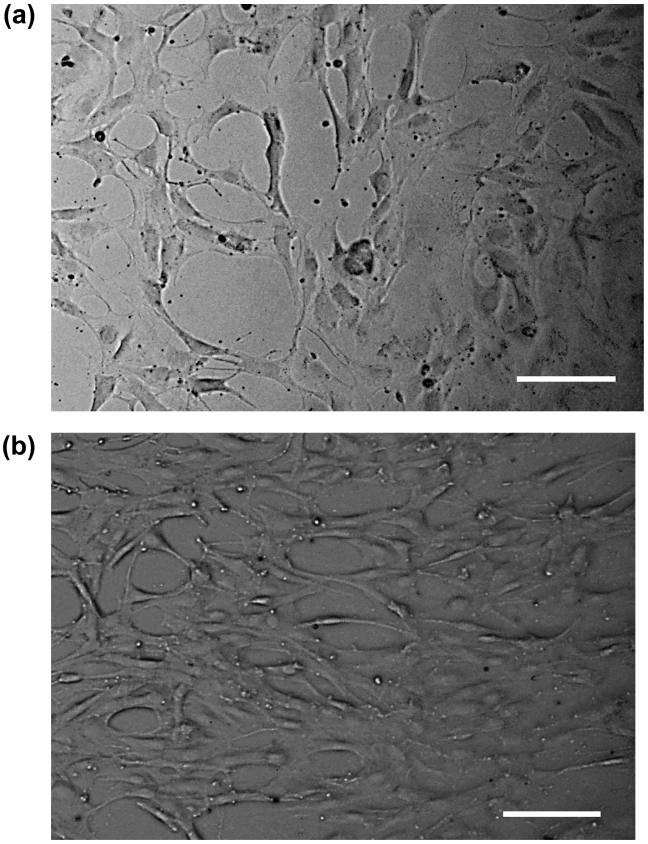

Figure 8. Optical micrographs of MC3T3-E1 cells (a) treated with fresh medium and (b) treated with medium containing the degradation products of ESO-A-DD5 at 10x magnification. Scale bar is 20 μm.

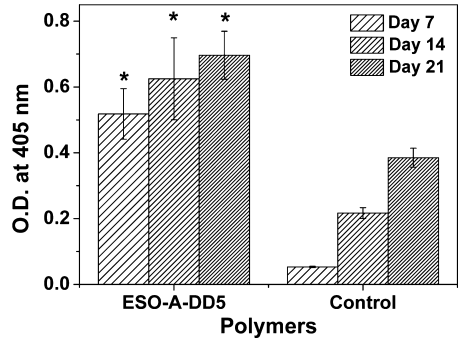

Figure 9. Quantification of mineral deposition on ESO-A-DD5 and control surfaces at day 7, day 14, and day 21. The * above the bars indicate that the samples are statistically significant when compared to the control. Data points represent mean ± SD (n = 3).

the osteogenic differentiation on the polymer surface as reported in other studies and this has been attributed to favorable adsorption at the surface.[67] In addition, as mentioned earlier, since ESO-A-DD5 possessed higher modulus, this polymer could have promoted enhanced osteogenic differentiation compared to control.

4. CONCLUSIONS

A library of PEAs was synthesized from soybean oil by modifying the molar ratios and changing the chain lengths of the monomers that resulted in polymers possessing a myriad of properties. Wide modulated modulus, degradation, release, and

DOI: 10.1021/acsami.6b10382
ACS Appl. Mater. Interfaces 2016, 8, 25170−25184

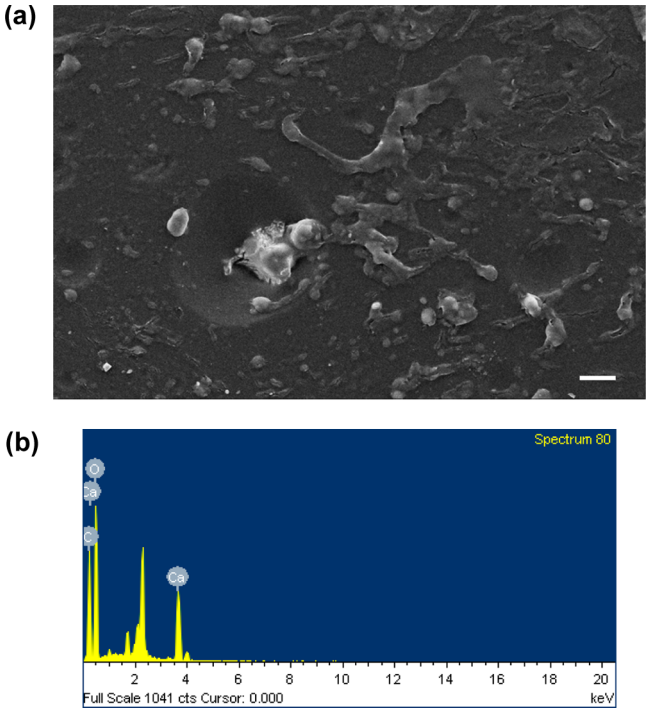

Figure 10. SEM micrographs coupled with EDS spectra of mineral deposited polymer discs (a) SEM micrograph of ESO-A-DD5 and (b) EDS spectra of ESO-A-DD5 (Magnification = 1.24 kX, scale bar = 10 μm).

cytocompatibility properties were obtained based on the variations in the synthesis. These polymers can be applicable in various applications depending on the circumstances. ESO-A-AA5 and ESO-A-SU5 possessed modulus of 15 and 18 MPa but exhibited a fast degradation of 24 h. This can be used in quick-release applications. ESO-A-SA5 demonstrated optimal modulus matching the moduli of cartilage and aortic valves[49] and slower degradation compared to many of the polymers investigated in this study. This polymer can be used for soft tissue engineering applications. ESO-A-DD5 showed a modulus of 120 MPa with very slow degradation. The results of osteogenic differentiation also demonstrated that these polymers are suitable candidates for bone tissue engineering. On the basis of the above observations, it may be concluded that ESO-A-DD5 can be employed for bone tissue engineering applications. The degradation and dye release followed first order kinetics and Higuchi kinetics, respectively. The rate of the degradation and dye release increases with decrease in modulus values, cross-linking density, and hydrophobicity and increase in %swelling.

■ ASSOCIATED CONTENT

Supporting Information

The Supporting Information is available free of charge on the ACS Publications website at DOI: 10.1021/acsami.6b10382.

Scheme S1. Chemical structure of rhodamine B and rhodamine B base. Figure S1. MALDI TOF MS of ESO (PDF)

■ AUTHOR INFORMATION

Corresponding Author

*Tel: 091-80-22933408. Fax: 091-80-23600472 E-mail: kchatterjee@chemeng.iisc.ernet.in (K.C.).

Notes

The authors declare no competing financial interest.

■ ACKNOWLEDGMENTS

This work was funded by the Department of Biotechnology (DBT), India (BT/PR5977/MED/32/242/2012). K.C. is grateful for Ramanujan fellowship from the Department of Science and Technology (DST), India. G.M. acknowledges the J.C. Bose fellowship from DST, India. J.N. would like to thank Mr. Shubham Jain and Dr. Jafar Hasan of Dept. of Materials Engineering for technical assistance regarding cell studies. We would also like to thank Ms. Vaishali A., Prof. S. Vasudevan of Inorganic and Physical Chemistry Dept and NMR Research Centre of IISc regarding NMR analysis. We acknowledge Proteomics facility, Molecular Biophysics Unit, IISc for MALDI TOF MS analysis.

■ REFERENCES

(1) Amini, A. R.; Laurencin, C. T.; Nukavarapu, S. P. Bone Tissue Engineering: Recent Advances and Challenges. *Crit. Rev. Biomed. Eng.* **2012**, *40*, 363−408.

(2) Porter, J. R.; Ruckh, T. T.; Popat, K. C. Bone Tissue Engineering: A Review in Bone Biomimetics and Drug Delivery Strategies. *Biotechnol. Prog.* **2009**, *25*, 1539−1560.

(3) Causa, F.; Netti, P. A.; Ambrosio, L. A Multi-Functional Scaffold for Tissue Regeneration: The Need to Engineer a Tissue Analogue. *Biomaterials* **2007**, *28*, 5093−5099.

(4) Babensee, J. E.; McIntire, L. V.; Mikos, A. G. Growth Factor Delivery for Tissue Engineering. *Pharm. Res.* **2000**, *17*, 497−504.

(5) Fonseca, A. C.; Gil, M. H.; Simões, P. N. Biodegradable Poly (Ester Amide)s−a Remarkable Opportunity for the Biomedical Area: Review on the Synthesis, Characterization and Applications. *Prog. Polym. Sci.* **2014**, *39*, 1291−1311.

(6) Rodriguez-Galan, A.; Franco, L.; Puiggali, J. Degradable Poly (Ester Amide)s for Biomedical Applications. *Polymers* **2011**, *3*, 65−99.

(7) Díaz, A.; Katsarava, R.; Puiggalí, J. Synthesis, Properties and Applications of Biodegradable Polymers Derived from Diols and Dicarboxylic Acids: From Polyesters to Poly (Ester Amide)s. *Int. J. Mol. Sci.* **2014**, *15*, 7064−7123.

(8) Asin, L.; Armelin, E.; Montané, J.; Rodríguez-Galán, A.; Puiggali, J. Sequential Poly (Ester Amide)s Based on Glycine, Diols, and Dicarboxylic Acids: Thermal Polyesterification Versus Interfacial Polyamidation. Characterization of Polymers Containing Stiff Units. *J. Polym. Sci., Part A: Polym. Chem.* **2001**, *39*, 4283−4293.

(9) Katsarava, R. In *Active Polycondensation: From Peptide Chemistry to Amino Acid Based Biodegradable Polymers*; Macromol. Symp., Wiley Online Library: 2003; pp 419−430.

(10) Karimi, P.; Rizkalla, A. S.; Mequanint, K. Versatile Biodegradable Poly (Ester Amide)s Derived from A-Amino Acids for Vascular Tissue Engineering. *Materials* **2010**, *3*, 2346−2368.

(11) Sun, H.; Meng, F.; Dias, A. A.; Hendriks, M.; Feijen, J.; Zhong, Z. A-Amino Acid Containing Degradable Polymers as Functional Biomaterials: Rational Design, Synthetic Pathway, and Biomedical Applications. *Biomacromolecules* **2011**, *12*, 1937−1955.

(12) Khan, W.; Muthupandian, S.; Farah, S.; Kumar, N.; Domb, A. J. Biodegradable Polymers Derived from Amino Acids. *Macromol. Biosci.* **2011**, *11*, 1625−1636.

(13) Tschan, M. J.-L.; Brulé, E.; Haquette, P.; Thomas, C. M. Synthesis of Biodegradable Polymers from Renewable Resources. *Polym. Chem.* **2012**, *3*, 836−851.

(14) Sharma, V.; Kundu, P. Condensation Polymers from Natural Oils. *Prog. Polym. Sci.* **2008**, *33*, 1199−1215.

(15) Desroches, M.; Escouvois, M.; Auvergne, R.; Caillol, S.; Boutevin, B. From Vegetable Oils to Polyurethanes: Synthetic Routes to Polyols and Main Industrial Products. *Polym. Rev. (Philadelphia, PA, U. S.)* **2012**, *52*, 38−79.

DOI: 10.1021/acsami.6b10382
ACS Appl. Mater. Interfaces 2016, 8, 25170−25184

(16) Pfister, D. P.; Xia, Y.; Larock, R. C. Recent Advances in Vegetable Oil-Based Polyurethanes. *ChemSusChem* **2011**, *4*, 703−717.
(17) Zhang, C.; Xia, Y.; Chen, R.; Huh, S.; Johnston, P. A.; Kessler, M. R. Soy-Castor Oil Based Polyols Prepared Using a Solvent-Free and Catalyst-Free Method and Polyurethanes Therefrom. *Green Chem.* **2013**, *15*, 1477−1484.
(18) Kris-Etherton, P. M.; Harris, W. S.; Appel, L. J.; Committee, A. N. Omega-3 Fatty Acids and Cardiovascular Disease New Recommendations from the American Heart Association. *Arterioscler., Thromb., Vasc. Biol.* **2003**, *23*, 151−152.
(19) Kamao, M.; Suhara, Y.; Tsugawa, N.; Uwano, M.; Yamaguchi, N.; UENISHI, K.; Ishida, H.; Sasaki, S.; Okano, T. Vitamin K Content of Foods and Dietary Vitamin K Intake in Japanese Young Women. *J. Nutr. Sci. Vitaminol.* **2007**, *53*, 464−470.
(20) Johnson, R. W.; Fritz, E. *Fatty Acids in Industry*; M. Dekker: New York, 1989.
(21) Tan, S.; Abraham, T.; Ference, D.; Macosko, C. W. Rigid Polyurethane Foams from a Soybean Oil-Based Polyol. *Polymer* **2011**, *52*, 2840−2846.
(22) Qin, Y.; Jia, J. R.; Zhao, L.; Huang, Z. X.; Zhao, S. W.; Zhang, G. W.; Dai, B. F. In *Synthesis and Characterization of Soybean Oil Based Unsaturated Polyester Resin, Advanced Materials Research*; Trans Tech Publications: Zürich, 2012; pp 349−353.
(23) Sonnenschein, M. F.; Ginzburg, V. V.; Schiller, K. S.; Wendt, B. L. Design, Polymerization, and Properties of High Performance Thermoplastic Polyurethane Elastomers from Seed-Oil Derived Soft Segments. *Polymer* **2013**, *54*, 1350−1360.
(24) La Scala, J.; Wool, R. P. Fundamental Thermo-Mechanical Property Modeling of Triglyceride-Based Thermosetting Resins. *J. Appl. Polym. Sci.* **2013**, *127*, 1812−1826.
(25) Even-Ram, S.; Artym, V.; Yamada, K. M. Matrix Control of Stem Cell Fate. *Cell* **2006**, *126*, 645−647.
(26) Campanella, A.; Bonnaillie, L.; Wool, R. Polyurethane Foams from Soyoil-Based Polyols. *J. Appl. Polym. Sci.* **2009**, *112*, 2567−2578.
(27) Wang, Z.; Zhang, X.; Wang, R.; Kang, H.; Qiao, B.; Ma, J.; Zhang, L.; Wang, H. Synthesis and Characterization of Novel Soybean-Oil-Based Elastomers with Favorable Processability and Tunable Properties. *Macromolecules* **2012**, *45*, 9010−9019.
(28) Miao, S.; Wang, P.; Su, Z.; Zhang, S. Vegetable-Oil-Based Polymers as Future Polymeric Biomaterials. *Acta Biomater.* **2014**, *10*, 1692−1704.
(29) Desroches, M.; Caillol, S.; Auvergne, R.; Boutevin, B.; David, G. Biobased Cross-Linked Polyurethanes Obtained from Ester/Amide Pseudo-Diols of Fatty Acid Derivatives Synthesized by Thiol−Ene Coupling. *Polym. Chem.* **2012**, *3*, 450−457.
(30) List, G.; Neff, W.; Holliday, R.; King, J.; Holser, R. Hydrogenation of Soybean Oil Triglycerides: Effect of Pressure on Selectivity. *J. Am. Oil Chem. Soc.* **2000**, *77*, 311−314.
(31) Nikolic, M. S.; Djonlagic, J. Synthesis and Characterization of Biodegradable Poly (Butylene Succinate-Co-Butylene Adipate) S. *Polym. Degrad. Stab.* **2001**, *74*, 263−270.
(32) Natarajan, J.; Madras, G.; Chatterjee, K. Maltitol-Based Biodegradable Polyesters with Tailored Degradation and Controlled Release for Bone Regeneration. *RSC Adv.* **2016**, *6*, 40539−40551.
(33) Raquez, J.-M.; Deléglise, M.; Lacrampe, M.-F.; Krawczak, P. Thermosetting (Bio) Materials Derived from Renewable Resources: A Critical Review. *Prog. Polym. Sci.* **2010**, *35*, 487−509.
(34) Kolanthai, E.; Sarkar, K.; Meka, S. R. K.; Madras, G.; Chatterjee, K. Copolyesters from Soybean Oil for Use as Resorbable Biomaterials. *ACS Sustainable Chem. Eng.* **2015**, *3*, 880−891.
(35) Lu, D.; Xiong, P.; Chen, P.; Huang, H.; Shen, L.; Guan, R. Preparation of Acrylic Copolymer Latex Modified by Fluorine, Silicon, and Epoxy Resin. *J. Appl. Polym. Sci.* **2009**, *112*, 181−187.
(36) Natarajan, J.; Rattan, S.; Singh, U.; Madras, G.; Chatterjee, K. Polyanhydrides of Castor Oil−Sebacic Acid for Controlled Release Applications. *Ind. Eng. Chem. Res.* **2014**, *53*, 7891−7901.
(37) Kumar, S.; Raj, S.; Kolanthai, E.; Sood, A. K.; Sampath, S.; Chatterjee, K. Chemical Functionalization of Graphene to Augment Stem Cell Osteogenesis and Inhibit Biofilm Formation on Polymer Composites for Orthopedic Applications. *ACS Appl. Mater. Interfaces* **2015**, *7*, 3237−3252.
(38) Bettinger, C. J.; Bruggeman, J. P.; Borenstein, J. T.; Langer, R. S. Amino Alcohol-Based Degradable Poly (Ester Amide) Elastomers. *Biomaterials* **2008**, *29*, 2315−2325.
(39) Coates, J. Interpretation of Infrared Spectra, a Practical Approach. In *Encyclopedia of Analytical Chemistry*; Meyers, R. A., Ed.; Wiley: Chichester, 2000; pp 10815−10837.
(40) Neto, P. R. C.; Caro, M. S. B.; Mazzuco, L. M.; da Graça Nascimento, M. Quantification of Soybean Oil Ethanolysis with 1h Nmr. *J. Am. Oil Chem. Soc.* **2004**, *81*, 1111−1114.
(41) Adhvaryu, A.; Erhan, S. Epoxidized Soybean Oil as a Potential Source of High-Temperature Lubricants. *Ind. Crops Prod.* **2002**, *15*, 247−254.
(42) Zhang, P.; Zhang, J. One-Step Acrylation of Soybean Oil (So) for the Preparation of So-Based Macromonomers. *Green Chem.* **2013**, *15*, 641−645.
(43) Rodríguez Galán, R. A.; Franco García, M. L.; Puiggalí Bellalta, J. Biodegradable Poly (Ester Amide)S: Synthesis and Applications. In *Biodegradable Polymers: Processing, Degradation and Applications*; Nova Science Publishers: Hauppauge, New York, 2011; Chapter 4, pp 207−272.
(44) Cheng, H.; Hill, P. S.; Siegwart, D. J.; Vacanti, N.; Lytton-Jean, A. K.; Cho, S. W.; Ye, A.; Langer, R.; Anderson, D. G. A Novel Family of Biodegradable Poly (Ester Amide) Elastomers. *Adv. Mater. (Weinheim, Ger.)* **2011**, *23*, H95−H100.
(45) Ahn, B.; Kim, S.; Kim, Y.; Yang, J. Synthesis and Characterization of the Biodegradable Copolymers from Succinic Acid and Adipic Acid with 1, 4-Butanediol. *J. Appl. Polym. Sci.* **2001**, *82*, 2808−2826.
(46) Montalvão, D.; Cláudio, R.; Ribeiro, A.; Duarte-Silva, J. Experimental Measurement of the Complex Young's Modulus on a Cfrp Laminate Considering the Constant Hysteretic Damping Model. *Compos. Struct.* **2013**, *97*, 91−98.
(47) Doyle, M. J. On the Effect of Crystallinity on the Elastic Properties of Semicrystalline Polyethylene. *Polym. Eng. Sci.* **2000**, *40*, 330−335.
(48) Bettinger, C. J.; Bruggeman, J. P.; Borenstein, J. T.; Langer, R. In Vitro and in Vivo Degradation of Poly (1, 3-Diamino-2-Hydroxypropane-Co-Polyol Sebacate) Elastomers. *J. Biomed. Mater. Res., Part A* **2009**, *91A*, 1077−1088.
(49) Barrett, D. G.; Yousaf, M. N. Design and Applications of Biodegradable Polyester Tissue Scaffolds Based on Endogenous Monomers Found in Human Metabolism. *Molecules* **2009**, *14*, 4022−4050.
(50) Anseth, K. S.; Shastri, V. R.; Langer, R. Photopolymerizable Degradable Polyanhydrides with Osteocompatibility. *Nat. Biotechnol.* **1999**, *17*, 156−159.
(51) Bruggeman, J. P.; de Bruin, B.-J.; Bettinger, C. J.; Langer, R. Biodegradable Poly (Polyol Sebacate) Polymers. *Biomaterials* **2008**, *29*, 4726−4735.
(52) Pasupuleti, S.; Madras, G. Synthesis and Degradation of Sorbitol-Based Polymers. *J. Appl. Polym. Sci.* **2011**, *121*, 2861−2869.
(53) Lips, P. A.; van Luyn, M. J.; Chiellini, F.; Brouwer, L. A.; Velthoen, I. W.; Dijkstra, P. J.; Feijen, J. Biocompatibility and Degradation of Aliphatic Segmented Poly (Ester Amide) S: In Vitro and in Vivo Evaluation. *J. Biomed. Mater. Res., Part A* **2006**, *76A*, 699−710.
(54) Barrett, D. G.; Luo, W.; Yousaf, M. N. Aliphatic Polyester Elastomers Derived from Erythritol and A, Ω-Diacids. *Polym. Chem.* **2010**, *1*, 296−302.
(55) Kim, J.; Lee, K.-W.; Hefferan, T. E.; Currier, B. L.; Yaszemski, M. J.; Lu, L. Synthesis and Evaluation of Novel Biodegradable Hydrogels Based on Poly (Ethylene Glycol) and Sebacic Acid as Tissue Engineering Scaffolds. *Biomacromolecules* **2008**, *9*, 149−157.
(56) Lange, H. Determination of the Degree of Swelling and Crosslinking of Extremely Small Polymer Gel Quantities by Analytical Ultracentrifugation. *Colloid Polym. Sci.* **1986**, *264*, 488−493.

DOI: 10.1021/acsami.6b10382
ACS Appl. Mater. Interfaces 2016, 8, 25170−25184

(57) Hong, W.; Jiao, W.; Hu, J.; Zhang, J.; Liu, C.; Fu, X.; Shen, D.; Xia, B.; Chang, Z. Periplasmic Protein Hdea Exhibits Chaperone-Like Activity Exclusively within Stomach Ph Range by Transforming into Disordered Conformation. *J. Biol. Chem.* **2005**, *280*, 27029−27034.
(58) Schneider, L. A.; Korber, A.; Grabbe, S.; Dissemond, J. Influence of pH on Wound-Healing: A New Perspective for Wound-Therapy? *Arch. Dermatol. Res.* **2007**, *298*, 413−420.
(59) Bueno Martínez, M.; Molina Pinilla, I.; Zamora Mata, F.; Galbis Pérez, J. A. Hydrolytic Degradation of Poly (Ester Amides) Derived from Carbohydrates. *Macromolecules* **1997**, *30*, 3197−3203.
(60) Erdmann, L.; Uhrich, K. E. Synthesis and Degradation Characteristics of Salicylic Acid-Derived Poly(Anhydride-Esters). *Biomaterials* **2000**, *21*, 1941−1946.
(61) Soppimath, K. S.; Aminabhavi, T. M.; Kulkarni, A. R.; Rudzinski, W. E. Biodegradable Polymeric Nanoparticles as Drug Delivery Devices. *J. Controlled Release* **2001**, *70*, 1−20.
(62) Korsmeyer, R. W.; Gurny, R.; Doelker, E.; Buri, P.; Peppas, N. A. Mechanisms of Solute Release from Porous Hydrophilic Polymers. *Int. J. Pharm.* **1983**, *15*, 25−35.
(63) Huang, X.; Brazel, C. S. On the Importance and Mechanisms of Burst Release in Matrix-Controlled Drug Delivery Systems. *J. Controlled Release* **2001**, *73*, 121−136.
(64) Soppirnath, K. S.; Aminabhavi, T. M. Water Transport and Drug Release Study from Cross-Linked Polyacrylamide Grafted Guar Gum Hydrogel Microspheres for the Controlled Release Application. *Eur. J. Pharm. Biopharm.* **2002**, *53*, 87−98.
(65) Shah, J. V. Cells in Tight Spaces: The Role of Cell Shape in Cell Function. *J. Cell Biol.* **2010**, *191*, 233−236.
(66) Wei, J.; Igarashi, T.; Okumori, N.; Maetani, T.; Liu, B.; Yoshinari, M. Influence of Surface Wettability on Competitive Protein Adsorption and Initial Attachment of Osteoblasts. *Biomed. Mater. (Bristol, U. K.)* **2009**, *4*, 045002.
(67) Kumar, S.; Raj, S.; Sarkar, K.; Chatterjee, K. Engineering a Multi-Biofunctional Composite Using Poly (Ethylenimine) Decorated Graphene Oxide for Bone Tissue Regeneration. *Nanoscale* **2016**, *8*, 6820−6836.

DOI: 10.1021/acsami.6b10382
ACS Appl. Mater. Interfaces 2016, 8, 25170−25184